Continuously Variable Inertance Tubes for Pulse Tube Refrigerators

J.M. Pfotenhauer[1], T. Steiner[1], L.M. Qiu[2]

[1]University of Wisconsin – Madison, Madison, WI 53706
[2]Zhejiang University, Hangzhou, 310027 P.R. China

ABSTRACT

The efficiency and cooling power of pulse tube refrigerators are highly dependent on the phase angle between the mass flow and pressure waves used to produce cooling. Inertance tubes are commonly used to set the phase angle for optimal efficiency. However, due to variations in fabrication or assembly, it is frequently unclear whether installed inertance tubes, with their fixed dimensions, produce the desired phase shift. A variable inertance tube allowing continuous adjustments to its geometry during operation has been constructed and mounted on a pulse tube, along with instrumentation to measure the pressure and mass flow oscillations and their relative phase at the interface between the inertance tube and pulse tube. A LabVIEW™-based lock-in amplifier enables real-time observation of the phase information. The variations in phase realized by changing the respective length and effective diameter of an inertance tube between 1.27 m to 1.55 m, and 6.52 mm to 6.61 mm, respectively, are compared to published models.

INTRODUCTION

Since the introduction of inertance tubes in the mid 1990's,[1,2] they have been widely used as an effective phase shift mechanism for pulse tube refrigerators. A variety of models[3-9] have been developed to quantitatively characterize the phase shift produced by the inertance tube. These models reveal that the phase shift is primarily dependent on the geometric parameters of inertance tube, namely its length and diameter as well as the size of the adjoining reservoir for a given level of acoustic power and frequency. Additional factors such as the transition geometry at the interface with the pulse tube refrigerator at one end, and with the reservoir at the other, as well as the assumed thermal interaction between the tube and its surroundings have received less attention. These factors also influence the phase shift provided by the inertance tube.

Modeling results[3,4] reveal that the phase angle produced by the inertance tube can be very sensitive to the length of the intertance tube in a range of tube lengths, and are fairly insensitive to the same parameter in other ranges of the length. The periodicity of this feature scales with the acoustic wavelength of the operating fluid (typically helium gas). Recognizing this sensitivity, and the importance to the pulse tube cooling power of the phase shift produced by the inertance tube, one may appreciate the advantage afforded by an inertance tube whose length could be continuously adjustable. Furthermore, it is possible that, the calculated phase shift for a specific inertance tube can be significantly different than that realized by the as-built version of the same tube due to various fabrication or assembly factors. Finally, as noted by previous authors,[10] the optimum phase

Cryocoolers 16, edited by S.D. Miller and R.G. Ross, Jr.

angle during the cool down of a pulse tube refrigerator is not typically the same as the optimum phase angle for steady state operation.

In view of the above issues, one can recognize the benefits that would accompany an easily adjustable inertance tube and the associated variable phase angle. However, the process of replacing one tube of a given length and diameter with another usually requires that the entire pulse tube refrigerator be first warmed to room temperature, depressurized, and disassembled. Following the replacement of one intertance tube with another, the system must be reassembled, evacuated, leak-checked, and repressurized before it can be re-cooled. In short, the process is involved and prohibitive. In order to avoid such complications, and to provide a means for adjusting the phase shift, we have developed a mechanism that allows real-time continuous adjustment of the inertance tube geometry while the pulse tube is operating.

As previously mentioned, an adjustable inertance tube has been fabricated and tested which enables a continuous variation of the phase shift in an operating pulse tube refrigerator. In the first section, details regarding the continuously adjustable inertance tube are provided along with a description of the mass flow meter and other components utilized in the verification test, including a LabVIEW-based lock-in amplifier. The second section describes the calibration procedure used for the mass flow meter, along with associated analyses correlating the mass flow rate to adiabatic pressure oscillations in the adjacent reservoir. The subsequent sections display the results of the continuously variable phase shift measurements and compare these to the inertance tube models.

EQUIPMENT

Several unique components have been developed to produce and measure the continuously variable phase-shift mechanism, including the adjustable inertance tube, a mass flow meter, and a LabVIEW™-based lock-in amplifier. After preparatory activities, these were assembled with a 2-stage pulse tube refrigerator to directly observe the influence of the variable inertance tube on the phase developed at the warm end of each pulse tube.

The adjustable inertance tube component uses a sliding tube-in-tube design as depicted in Fig. 1. Here the smaller tube's dimensions, along with those of the two adjacent larger tubes are listed in Table 1. One of the larger tubes connects to the mass flow meter, while the other connects to the reservoir. In order to minimize the flow of gas into and out of the annular gap between the tubes, a 0.3 mm thick x 10 mm long layer of indium is applied to the outer diameter at one end of the inner tube. The leak-free seal between the pressurized tubes and the surrounding environment is realized by trapping a single Viton O-ring between two flanges, with a groove designed to squeeze the O-ring down around the inner tube. A threaded rod is used to hold the tubes together under pressure,

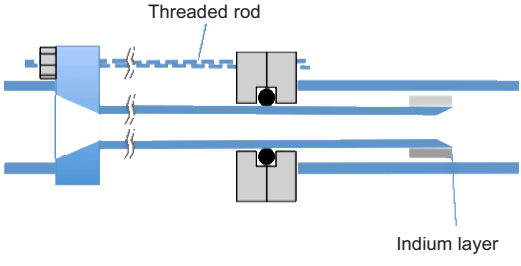

Figure 1. Schematic of telescoping embodiment of continuously variable inertance tube

Table 1. Geometric Parameters of Variable Inertance Tube Components

	Outer diameter (mm)	Inner diameter (mm)	Length (m)
Outer Tube 1	9.53	7.04	0.356
Inner Tube	6.53	4.83	0.327
Outer Tube 2	9.53	7.04	0.886

and also allows for 27 cm of continuous length adjustment, giving the inertance tube a range of total lengths from 0.127 m to 0.154 m.

The mass flow meter is constructed by stacking 110 copper screens (200 mesh) into the space between two conflat flanges as depicted in Fig. 2. The pressure drop through the screen pack is dominated by the flow resistance and measured using two separate Endevco (model 8510B-500) pressure transducers mounted at each end of the screen pack. The dimensions of the screen pack are 11.7 mm long x 12.7 mm diameter.

For future use, the mass flow meter has been calibrated so that the amplitude of the pressure drop across the screen pack can be directly related to a mass flow rate. For this purpose, the mass flow meter is mounted on the output of a linear compressor, (60 Amp Q Drive model 2S297W TwinSTAR Pressure Wave Generator) and connected on its opposite side, to a 0.5 liter reservoir volume instrumented with a third Endevco pressure transducer. Through the assumption of adiabatic flow into and out of the reservoir, the mass flow rate may be related to the pressure in the reservoir *p(t)*. Beginning with an energy balance around the reservoir, the mass flow rate into and out of the reservoir is related to the resulting adiabatic temperature rise of the gas in the reservoir according to:

$$m(t)c_v T(t) - m_0 c_v T_0 = (m(t) - m_0)c_p T_{i/o}(t) \tag{1}$$

Here m(t) and m_o are respectively the mass in the reservoir at a time t, and the average value, c_v and c_p are the specific heat at constant volume and constant pressure respectively, T(t) is the time dependent gas temperature in the reservoir, and $T_{i/o}(t)$ is the temperature of the gas coming in (i) or going out (o) of the reservoir. Note that although the temperature of the incoming gas may be constant (T_o), that of the gas going out will vary with the adiabatic temperature in the reservoir (T(t)). From Eq. (1) one may obtain expressions for the mass flow rate into and out of the reservoir,

$$if\ \dot{m} > 0;\quad \dot{m} = m_0 \frac{d\left[\dfrac{T_0 - \gamma T_0}{T(t) - \gamma T_0}\right]}{dt} = m_0 \frac{(1-\gamma)T_0}{\left[T(t) - \gamma T_0\right]^2}\frac{dT(t)}{dt} \tag{2a}$$

$$if\ \dot{m} < 0;\quad \dot{m} = m_0 \frac{d\left[\dfrac{T_0 - \gamma T(t)}{T(t) - \gamma T(t)}\right]}{dt} = \frac{m_0}{1-\gamma}\frac{d\left[\dfrac{T_0}{T(t)} - r\right]}{dt} = \frac{m_0 T_0}{1-\gamma} T(t)^{-2}\frac{dT(t)}{dt} \tag{2b}$$

Here positive flow is defined as from the compressor toward the reservoir. Combining these equations with the ideal gas law and a sinusoidal pressure assumption, one obtains

$$when\ \dot{m}>0;\quad \dot{m} = -m_0 \frac{(1-\gamma)^2}{\gamma}\frac{\omega P_d}{P_0}\frac{\left(1+\dfrac{P_d}{P_0}\sin\omega t\right)^{-1/\gamma}}{\left[\left(1+\dfrac{P_d}{P_0}\sin\omega t\right)^{(\gamma-1)/\gamma} - \gamma\right]^2}\cos(\omega t) \tag{3a}$$

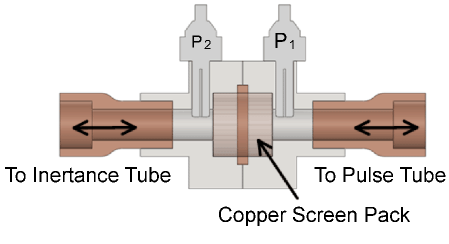

Figure 2. Schematic of mass flow meter

$$when\ \dot{m}<0;\quad \dot{m} = -\frac{m_0}{\gamma}\frac{\omega P_d}{P_0}\left(1+\frac{P_d}{P_0}\sin\omega t\right)^{\left(\frac{1}{\gamma}-2\right)}\cos(\omega t) \tag{3b}$$

Fig. 3 compares the mass flow calculated from Eq. (3a) with that calculated from the approximation relation

$$\dot{m}_2 = P_d\omega\cos(\omega t)\frac{vol}{\gamma R_{he}T_0} \tag{4}$$

and reveals a small difference in both phase and amplitude between the approximate and full solution. Eqns. (3a) and (3b) have been used in the subsequent mass flow calibration.

The results of the calibration at 27 Hz and for two different values of average pressure are displayed in Fig. 4. The difference in pressure amplitude across the flow meter, P_1-P_2 = ΔP, was measured for a large range of compressor power, with pressure differences ranging from 0.25 to 1.2 bar, and resulting mass flows ranging from 3.5 to 17.5 g/s. A 2nd order polynomial of mass flow vs. pressure difference was found to very closely fit the calibration data in each case.

A lock-in amplifier, developed entirely within LabVIEW™ 8.6, and based off the LabVIEW™ Lock-in Start-up kit, available from National Instruments (NI), has been used to measure the phase

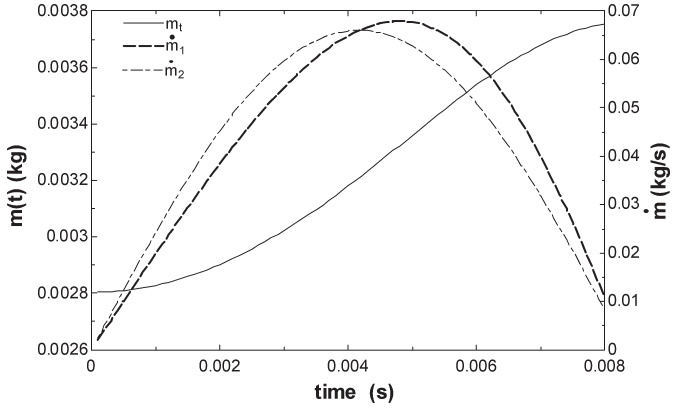

Figure 3. Comparison of adiabatic mass flow rate calculations according to Eq. (3a) - $\dot{m}_1$ and Eq. (4) - $\dot{m}_2$, for mass flow entering the reservoir. The mass increase in the reservoir m(t) is from Eq. (3a).

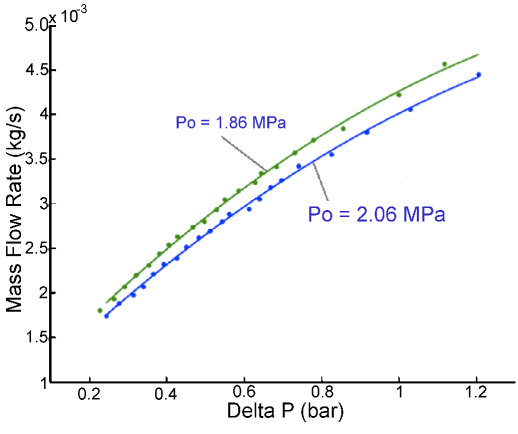

Figure 4. Calibration data for mass flow meter at two different average pressures

difference between the pressure and mass flow oscillations. This kit was modified to include the newer NI DAQmx drivers, to use the pressure P_1 as the reference and the difference in pressures P_1-P_2 across the screen pack as the signal, and to enable data storage to an external file for subsequent analysis. Additional modifications include conversions from voltage to pressure and from pressure drop to mass flow rate, as well as an option to record the input oscillation data.

A 14-bit NI USB-6009 low-cost DAQ was used for data acquisition. This device includes four analog inputs, allowing a quick switch between mass flow meters during operation in software. 10,000 samples were collected at a sampling frequency of 10 kHz, resulting in one second's worth of data being used to define the phase and amplitude results.

PHASE SHIFT MEASUREMENTS

Two identical calibrated mass flow meters as described above have been installed between the warm ends of each pulse tube in a two-stage pulse tube refrigerator and identical adjustable inertance tubes also as described above. The pulse tube was originally designed to provide 10's of watts at 80 K and is driven by an 80 Amp Q Drive model 2S297W TwinSTAR Pressure Wave Generator. However, due to multiple reasons, not the least of which being that the calibrated mass flow meters introduce an inappropriately large flow impedance (a feature to be corrected in future embodiments), the designed operation of the pulse tube was not achieved. In fact, during the present tests, the voltage signal from the thermometer at the cold end of the second stage was only monitored to identify steady state conditions.

At steady state conditions, the average pressure in the pulse tube was established at 1.789 MPa, and phase shift measurements were gathered at both 27 Hz and 40 Hz. Due to the large resistance across the mass flow meters, the pressure amplitude in the inertance tubes was reduced to approximately 13.6 kPa. The LabVIEW™ Lock-in amplifier was used to determine the phase difference between the pressure oscillation on the pulse tube side of the mass flow meter, and the mass flow oscillation through the meter. By changing the length of the adjustable inertance tube, phase information was gathered over the range of lengths from 1.27 m to 1.55 m. The results are shown in Fig. 5.

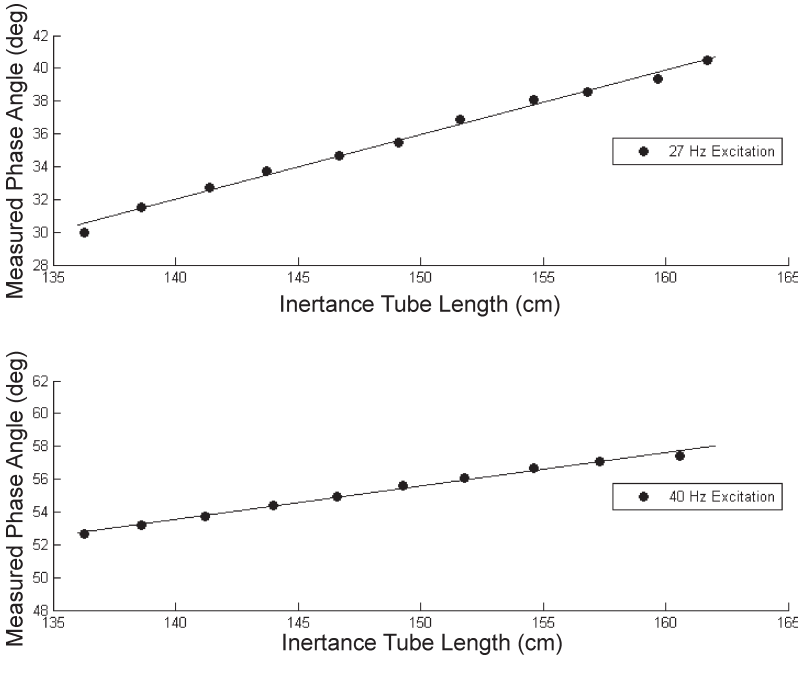

Figure 5. Phase shift resulting from change in inertance tube length

A nearly linear change in phase results from the change in the inertance tube length. For 27 Hz operation, the 0.28 m length change results in a phase change of roughly 12", while for 40 Hz operation, the phase change resultant from the same change of inertance tube is reduced to 5.

Note that because the fraction of length for which the inner diameter is 4.83 mm vs. 7.04 mm also changes as the tube length is modified, both the length and effective inner diameter of the inertance tube are changed in these measurements. The change in averaged diameter is from 6.52 mm to 6.61 mm.

Various features of the data displayed in Fig. 5 have also been confirmed through the use of a distributed component model.[4] The model has been modified to include the three different inertance tube dimensions defined in Table 1, incorporated into a single tube. For the same change in lengths used in the measurements, the model displays a linear change in the phase shift by approximately 35 degrees at 27 Hz and by approximately 7 degrees at 40 Hz.

SUMMARY

A device enabling continuous run-time changes to the phase angle between the pressure and flow oscillations in a pulse tube refrigerator has been demonstrated. The changes are made possible through an adjustable inertance tube, whose length and effective diameter can be continuously changed. The phase measurements are gathered using a packed-screen mass flow meter, pressure transducers, and a LabVIEW™ based lock-in amplifier. Further explorations with, and improvements to, the phase shifter are anticipated.

ACKNOWLEDGMENTS

The authors thank Steve Meitner for fabrication of the variable inertance tube and mass flow meters.

REFERENCES

1. Zhu, S.W., Zhou, S.L., Yoshimura, N., and Matsubara, Y., “Phase Shift Effect of the Long Neck Tube for the Pulse Tube Refrigerator,” *Cryocoolers 9*, Plenum Press, New York, (1996), pp. 269-278.
2. Gardner, D.L., and Swift, G.W., “Use of Inertance in Orifice Pulse Tube Refrigerators,” *Cryogenics* Vol. 37, Issue 2, 1997, pp. 117-121.
3. Luo, E., Radebaugh, R., and Lewis, M., “Inertance Tube Models and their Experimental Verification,” *Adv. in Cryogenic Engineering*, Vol. 49B, Amer. Institute of Physics, Melville, NY (2004), pp. 1485-1492.
4. Schunk, L.O., Nellis, G.F., and Pfotenhauer, J.M., “Experimental Investigation and Modeling of Inertance Tubes,” *Journal of Fluids Engineering*, vol. 127, no. 5, (2005), pp.1029-1037.
5. Dodson, C., Lopez, A., Roberts, T. and Razani, A., “A model for the parametric analysis and optimization of inertance tube pulse tube refrigerators,” *Adv. in Cryogenic Engineering*, Vol. 53, Amer. Institute of Physics, Melville, NY (2008), pp. 685-692.
6. Flake, B. and Razani, A., “Phase shift and compressible fluid dynamics in inertance tubes,” *Cryocoolers 13*, Kluwer Academic/Plenum Publishers, New York (2005), pp. 275-284.
7. Lewis, M., Bradley, P. and Radebaugh, R., “Impedance measurements of inertance tubes,” *Adv. in Cryogenic Engineering*, Vol. 51, Amer. Institute of Physics, Melville, NY (2006), pp. 1557-1563.
8. Gustafson, S., Flake, B., Razani, A., “CFD Simulation of oscillating flow in an inertance tube and its comparison to other models,” *Adv. in Cryogenic Engineering*, Vol. 51, Amer. Institute of Physics, Melville, NY (2006), pp. 1497-1504.
9. Radebaugh, R., Lewis, M.A., Luo, E., Pfotenhauer, J.M., Nellis, G.F., and Schunk, L.O., “Inertance Tube Optimization for Pulse Tube Refrigerators,”*Adv. in Cryogenic Engineering*, Vol. 51, Amer. Institute of Physics, Melville, NY (2006), pp. 59-67.
10. Radebaugh, R., O’Gallagher, A., Lewis, M.A., and Bradley, P.E., “Proposed Rapid Cooldown Technique for Pulse Tube Refrigerators,” Cryocoolers 14, ICC Press, Boulder, CO (2007), pp. 231-240.